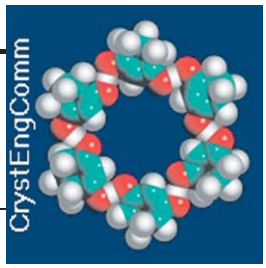

Paper

A co-crystal containing Kemp's tri-acid and acetic acid: a 0D aggregate disrupts a thermodynamically preferred 1D rod motif†

Scott L. Childs*‡ and Karl S. Hagen

Department of Chemistry, Emory University, Atlanta, GA 30322, USA.
E-mail: childs@euch3i.chem.emory.edu; khagen@emory.edu

Received 6th March 2002, Accepted 1st May 2002
Published on the Web 16th July 2002

A supramolecular aggregate of two Kemp's tri-acid (*cis*,*cis*-1,3,5-trimethylcyclohexane-1,3,5-tricarboxylic acid, KTA) and four acetic acid molecules is arranged in a centrosymmetric zero-dimensional (0D) motif (**2**). This unusual pairing of unlike carboxylic acids disrupts a 1D hydrogen-bonded rod motif that is thermodynamically preferred by KTA (**1**) under most conditions. The six-molecule 0D aggregate reported here behaves like a large molecule with excellent self-recognition properties. Efficient centrosymmetric packing leads to maximized van der Waals contact and multiple C–H···O interactions between aggregates. The synthesis and physical properties of the parent KTA rod structure (**1**) and the acetic acid co-crystal (**2**) are compared and discussed.

Introduction

Molecules can be crystallized in a number of ways. Crystallizing different forms of the same molecule can generate a library of additional structures. For instance, inorganic chemists exchange counter ions to isolate new salts. Analyzing the resulting family of salts reveals additional information about the coordination compound common to all of the structures.[1] This strategy can be applied to any system in which the molecule of interest can be crystallized with some other molecular species in order to yield a unique structure.

There are a number of terms that describe this class of structures: solvate, salt, clathrate, host–guest compound, inclusion compound, 1 : 1 addition compound, binary or ternary crystal, hydrate, and coordination complex. All of these can be classified under the single term 'co-crystal' because they all describe ways of creating unique crystal structures that contain a selected species plus some other molecular component. This strategy is an important tool to the crystal engineer because it allows a molecule to be studied in different solid-state environments where each structure will have distinctive physical characteristics and unique non-bonded interactions.[2]

We have applied this approach in our studies of the solid state properties of Kemp's tri-acid[3] (*cis*,*cis*-1,3,5-trimethylcyclohexane-1,3,5-tricarboxylic acid, KTA, Fig. 1). This is part of a series of papers that is exploring the properties and interactions of KTA co-crystals.[4] The example given in this paper demonstrates how KTA is co-crystallized with acetic acid to form $[(Me_3C_6H_6(COOH)_3)(MeCOOH)_2]_2$ (**2**).

Results and interpretation

The focus of this paper will be on comparing the co-crystal, **2**, with the structure of KTA, $[Me_3C_6H_6(COOH)_3]$ (**1**). For simplicity, **2** can be described as a 'host–guest' system in which the structure of **1** is considered to be the 'host' structure, and **2** contains the KTA host molecule and the acetic acid guest. This emphasizes the fact that KTA is contained in both structures and is the central molecule of interest. The result is two different structures that both contain KTA, but which have very different physical properties.

Kemp's tri-acid – a molecular building block

Kemp's acid, a facial amphiphile, is the molecular building block used in this study. Structural information on KTA was first published (without coordinates) by Rebek Jr. *et al.* in 1985.[5] Rebek noted that the potential C_3 rotational symmetry was not carried into the crystal structure and that the strong hydrogen bonding pattern formed a rod motif. The structure (with coordinates) has subsequently been reported;[6] however, we have chosen to report an additional set of coordinates for **1** obtained from data collected under the same conditions as **2** (100 K using a CCD detector).

Crystal structure comparison

A helpful way to visualize and understand a complicated crystal structure is to break down the packing motifs into low-dimensional substructures (see the KAP method of Perlstein and co-workers[7]). In **1** and **2**, the strong hydrogen bonds form supramolecular aggregates of KTA. In **1** the motif is a 1D rod, whereas **2** forms a zero-dimensional (0D) aggregate (Fig. 2). These low-dimensional substructures are packed together to form complete 3D structures.

The KTA rod structure, **1**, crystallizes with a dominant 1D rod motif formed by the familiar carboxylic acid pair hydrogen bonding. It is a consistent and persistent motif that dominates

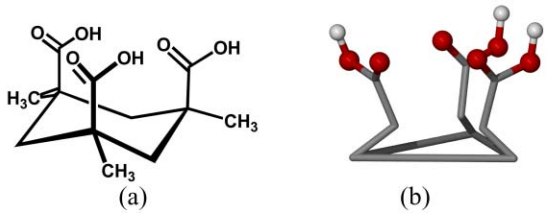

Fig. 1 (a) Kemp's tri-acid, KTA. (b) A simplified view of KTA that is used for clarity; click image or here to access a 3D representation. Actual crystal coordinates are used for the acid groups, and the triangle represents the three methyl groups.

†Based on the presentation given at CrystEngComm Discussion, 29th June–1st July 2002, Bristol, UK.
‡Current address: Design Science Research, Atlanta, GA, USA (a subsidiary of SSCI, Inc., West Lafayette, IN, USA).

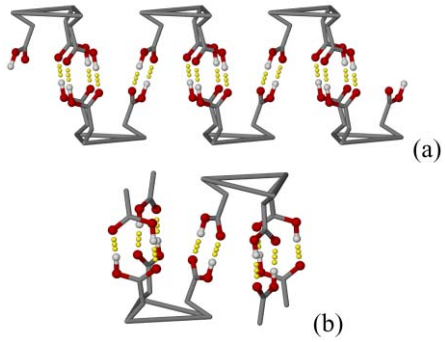

Fig. 2 (a) KTA preferentially forms a one-dimensional (1D) rod motif in **1**; click image or here to access a 3D representation. (b) The zero-dimensional (0D) aggregate of **2**; click image or here to access a 3D representation.

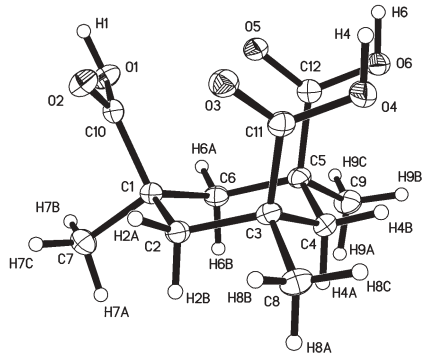

Fig. 4 Thermal ellipsoid plot (50% probability level) for **1**.

this system. Each KTA molecule attaches to neighboring molecules through the strong O–H···O hydrogen bonds *via* single and double pairs of carboxylic acids, forming a robust, 1D rod motif with $P\bar{1}$ rod group symmetry. Inversion centers are located in the center of the single acid pair and in between the double pair of acid groups along the *a* axis.

The 0D aggregate in **2** can be seen as a 'truncated rod' in which the pair of acid groups that would be used to extend the 1D motif have been capped off by the acetic acid molecules. Thus, the acetic acid 'guest' molecules have interrupted the 1D rod motif, although the structural organization of **2** remains similar to the parent rod structure, **1** (Fig. 3).

Both structures crystallize in the $P2_1/n$ space group and, somewhat surprisingly, the supramolecular organization of **2** mimics that of the parent structure **1** (Fig. 4) in that the aggregates of **2** (Fig. 5) are packed with the KTA molecules organized as a pseudo-rod that mirrors the direction of the rod

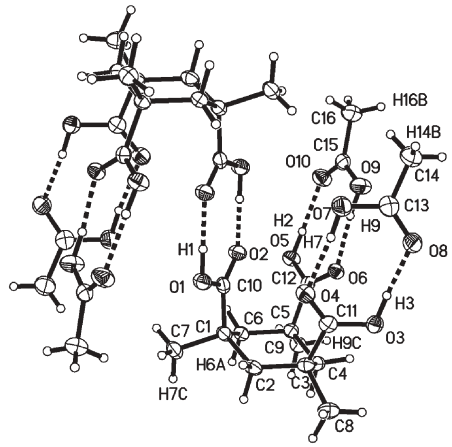

Fig. 5 Thermal ellipsoid plot (50% probability level) for **2**. Only hydrogen atoms involved in O–H···O or C–H···O interactions are labeled.

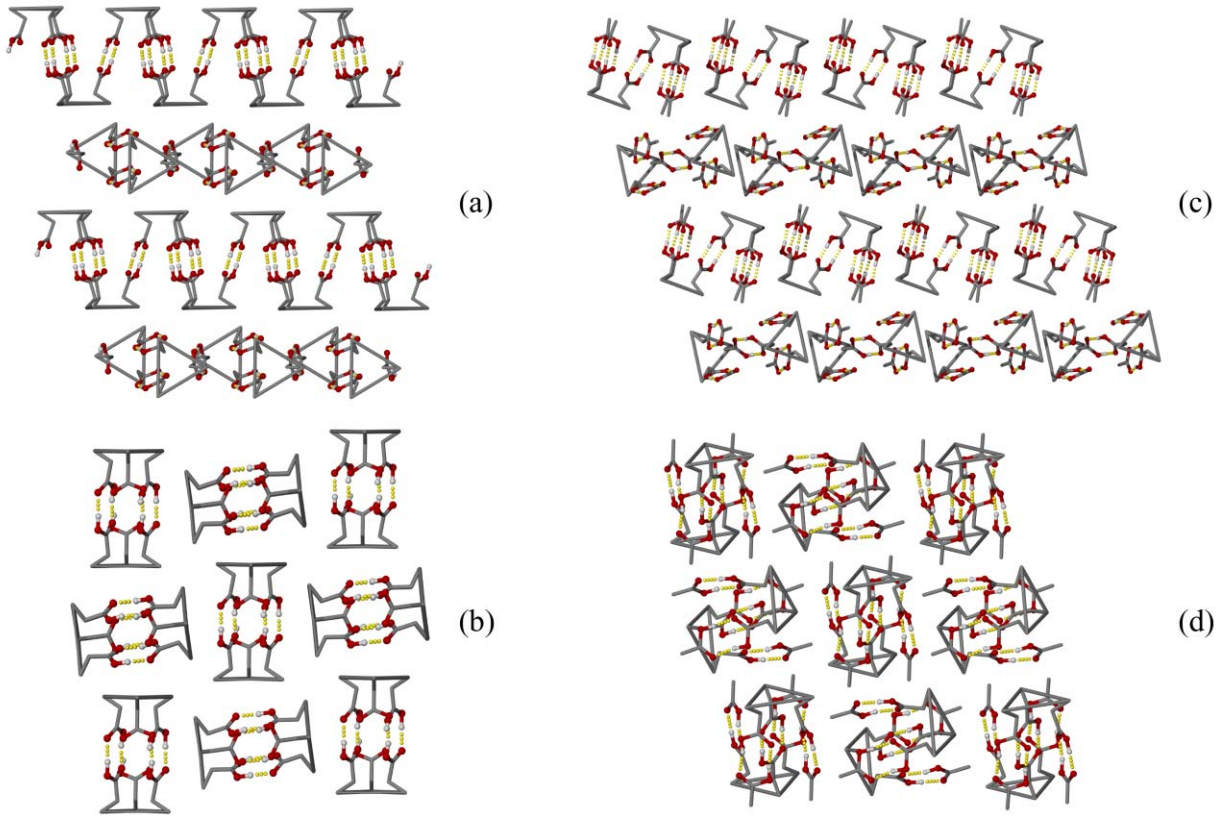

Fig. 3 Packing diagrams for **1** are shown in (a) and (b), and **2** is depicted in (c) and (d). The rod from **1** and the pseudo-rod from **2** extend along the *a* axis, which is horizontal in (a) and (c) and normal to the *bc* plane shown in (b) and (d). Click image (b) or here to access a 3D representation. Click image (c) or here to access a 3D representation.

motif in **1**. The six-molecule aggregate is arranged along the *a* axis and is stacked in a way analogous to its parent structure (Fig. 3).

The inversion center packing in **2** is identical to the organization of **1** in that one inversion center is located in the center of an acid pair, and a second inversion center is placed so as to extend the rod substructure. However, the second inversion center is placed within the rod substructure in **1** and between the aggregates in **2**.

The packing of the rods in **1** and the pseudo-rods in **2** is accomplished by organizing them in a co-linear fashion as shown in Fig. 3. The rods are crystallographically related by inversion symmetry, but also by an *n* glide that accompanies the $P2_1/n$ space group. The rods in both **1** and **2** are arranged in a roughly orthogonal manner, meaning that neighboring rods are related (non-crystallographically) by a translation and a rotation of 90° when looking down the *a* axis in a view of the *bc* plane (Fig. 6).

Analysis of non-bonded interactions

The interactions that stabilize these structures are a balance between strong O–H···O hydrogen bonds, weak C–H···O hydrogen bonds, and van der Waals forces. The more robust O–H···O interactions form the 1D structure-directing rod motif in **1**, but they do not play a significant role in the stabilization of **2** as a whole. Instead they form stable 0D supramolecular substructures that are used as building blocks to construct the full 3D array. In fact, we think of the 0D aggregate in **2** as a distinct molecular packing unit with 'intramolecular' O–H···O hydrogen bonds. These 0D aggregates interact in the 3D array only by the concerted interactions of the C–H···O and van der Waals interactions. This is not the case in **1**, where the strong O–H···O interactions are extended into a 1D substructure that forms the underlying structural motif.

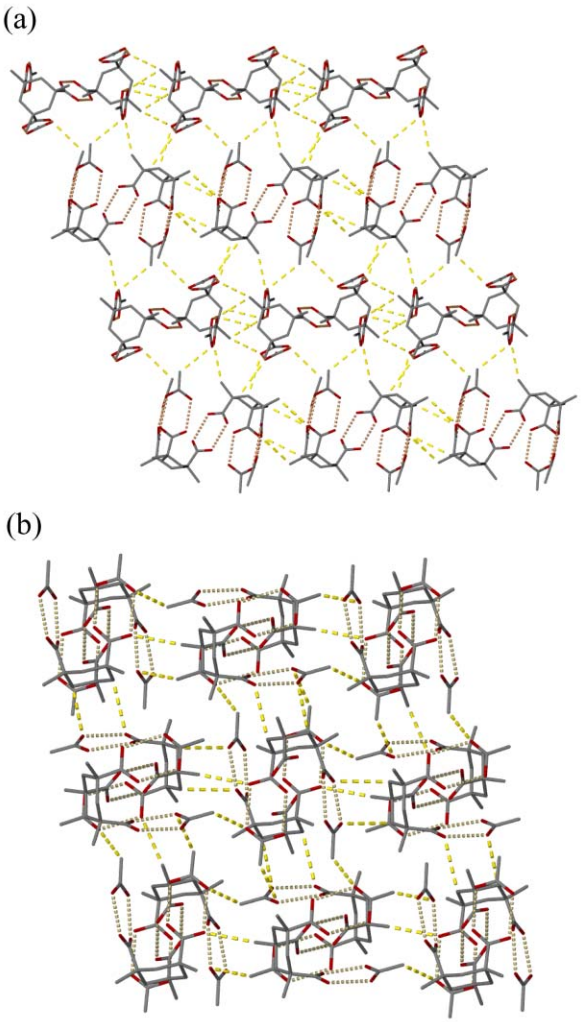

Fig. 6 (a) The *ac* plane in **2** is shown with the pseudo-rod *a* axis horizontal. (b) The packing motif in the *bc* plane in **2** is depicted in this cross-section of the stacked 2D layers. Both (a) and (b) include the C–H···O interactions (in yellow) between the aggregates.

There are secondary acceptor sites on the oxygen atoms of the acid groups involved in the strong O–H···O hydrogen bonding. These are accessible on the outer surface of the aggregate and function as acceptor sites for lateral intra-aggregate C–H···O interactions. The availability of these sites on the surface of the very uniformly shaped 0D aggregate, combined with the self-complementary surfaces of the aggregate, result in numerous C–H···O interactions. These weak interactions, acting in concert with the summed van der Waals forces, are able to stabilize the structure so that under very specific conditions the co-crystal is formed instead of the thermodynamically preferred rod form of KTA.

In **1** there are no C–H···O interactions with H···O distances below 2.5 Å (using normalized C–H distances), whereas in **2** there are four such interactions (see Table 1). There are five additional C–H···O contacts in **2** if an H···O distance of 2.9 Å is allowed, all with C–H···O angles between 138 and 148°.

Attributing the stabilization of **2** only to the concerted C–H···O interactions would be incomplete because our understanding of the role of these interactions in crystal packing is still being developed, and also because the analysis of **2** presents no clear C–H···O synthon acting as a structure-directing influence. Additional clues about how **2** manages to compete with **1** can be gleaned from examining the role of the van der Waals interactions, which are the only other interactions that share in the responsibility of stabilizing the intra-aggregate interactions. This qualitative assessment is summarized graphically in Fig. 7. The very regular shape of the aggregate assists directly in the efficient packing of the aggregate because the surface of the aggregate has no significant 'bumps' that would disrupt the complementary surface-to-surface interactions.

We believe that the very regular shape of the 0D aggregate plays a significant role in the stabilization of **2**. The space-filling representation of the aggregate in Fig. 7 shows that the four acetic acids and two KTA molecules assemble into a regular box-like shape. This facilitates the packing of the aggregates in the lattice. We were not able to isolate a co-crystal similar to **2** using other small carboxylic acids. We tested formic, propionic, isobutyric, 2,2-dimethylpropionic, butyric, 3-methylbutyric (isovaleric), *tert*-butylacetic, and benzoic acids, as well as various substituted benzoic acid derivatives. This suggests that the basic shape of the aggregate is a significant influence in the formation of **2**.

Comparing physical properties

Braga *et al.* suggest that "the ultimate goal is that of making crystals with a purpose".[8] This indicates that the physical properties of engineered crystals should be examined and reported so that we can begin more rigorously to correlate theory and analysis with the physical properties of the resulting molecular materials.[9] Correlating internal organization and observations of bulk physical properties is a simple and effective method of characterizing a material.

Grown at thermodynamic equilibrium in a neutral solvent such as ethanol, the basic morphology of the KTA crystals, **1**, reflects the internal molecular organization (Fig. 8). The morphology is a rod, just like the stable molecular aggregates of KTA that form the crystal itself. The morphology also

Table 1 Selected close contacts in **1** and **2**. All contacts use normalized hydrogen distances (0.983 Å for O–H and 1.083 Å for C–H). All O–H···O contacts are between carboxylic acids. The cutoff distance for C···O interactions is 2.75 Å and the C–H–O angle must be greater than 110°

O–H···O hydrogen bonds in **1**					
Donor	Acceptor	Hydrogen	O···O/Å	H···O/Å	O–H–O/°
O4	O5	H4	2.625	1.655	168
O6	O3	H6	2.681	1.699	176
O1	O2	H1	2.625	1.663	169
C–H···O hydrogen bonds in **1**					
Donor	Acceptor	Hydrogen	C···O/Å	H···O/Å	C–H–O/°
C8	O1	H8A	3.581	2.564	156
C7	O5	H7A	3.680	2.721	147
O–H···O hydrogen bonds in **2**					
Donor	Acceptor	Hydrogen	O···O/Å	H···O/Å	O–H–O/°
O1	O2	H1	2.601	1.618	177
O3	O8	H3	2.648	1.699	174
O5	O10	H5	2.683	1.701	177
O7	O4	H7	2.675	1.696	173
O9	O6	H9	2.651	1.672	173
C–H···O hydrogen bonds in **2**					
Donor	Acceptor	Hydrogen	C···O/Å	H···O/Å	C–H–O/°
C14	O10	H14B	3.350	2.434	141
C6	O3	H6A	3.483	2.405	173
C9	O6	H9C	3.462	2.474	151
C16	O10	H16A	3.562	2.483	174
C7	O5	H7C	3.178	2.554	116
C16	O7	H16B	3.502	2.615	139
C9	O3	H9C	3.622	2.747	138

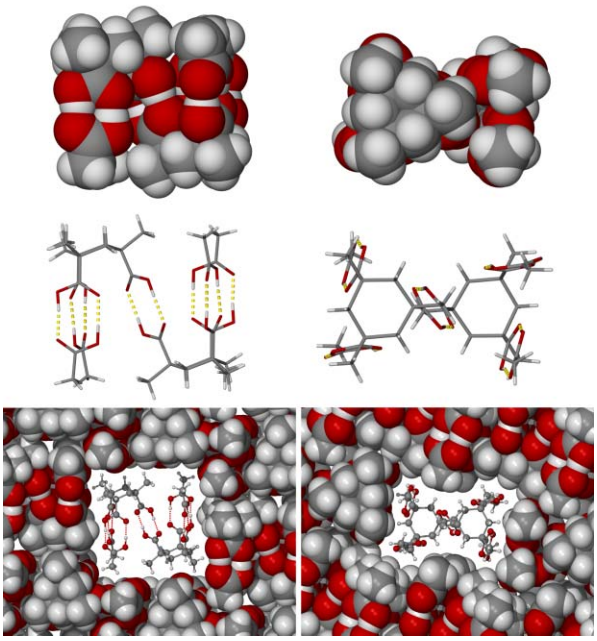

Fig. 7 Orthogonal views of a single aggregate in cylinder and space-filling depictions highlight the self-complementary packing in **2**. The bottom image shows a ball and stick aggregate inside of an *ac* layer that is viewed in space-filling mode. The aggregate, shown in the top two images, packs into this regularly shaped cavity with excellent self-recognition, allowing the C–H···O interactions close approach and the van der Waals interactions to share maximum surface area.

reflects the internal symmetry of the space group $P2_1/n$ with the rod extending along the *a* axis. An imposed mirror plane and two-fold rotation are also reproduced in the morphology.

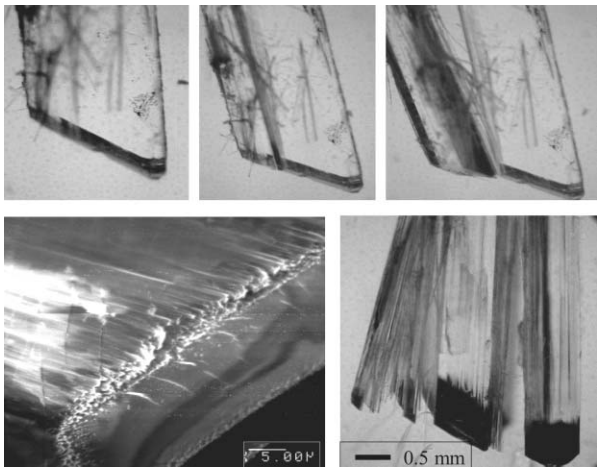

Fig. 8 Physical properties of the KTA rod crystals, **1**. The intact KTA rod crystal is shown in the image on the upper left. A single cut is made along the rod axis of the crystal (top middle). The crystal cleaves relatively cleanly and the cut faces are parallel to the sides of the crystal and orthogonal to the axis of the hydrogen-bonded rods. Cleaving the crystal perpendicular to the rod axis produced the results shown in the bottom right image. The rod shatters and forms many small rods. The effect of dissolving a crystal of KTA in methanol is shown in the bottom left image. The crystal was soaked for 2 min, isolated, dried and imaged at 5 kV in SEM after being coated with 10 nm of 60 : 40 Au : Pd.[10] As the crystal dissolves, the rod axis is evident.

When crystals of **1** are crushed with the point of a probe, the crystal shatters along the long axis of the crystal and forms a multitude of smaller, well defined rods. The internal hydrogen bonding in the structure correlates with the preferred axis of cleavage. The acetic acid co-crystal, **2**, cleaves irregularly, indicating the lack of strong directional bonding in the crystal.

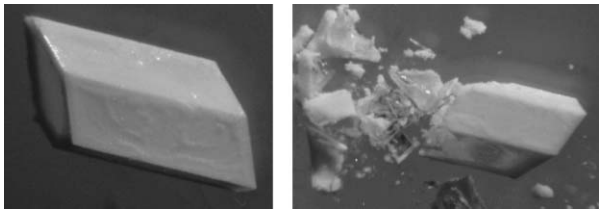

Fig. 9 Physical properties of the KTA–HOAc co-crystal, **2**. The image on the left shows a crystal of **2** that has been exposed to the air. The image on the right shows the same crystal after being crushed with the point of a probe.

Synthesis of **1** is a straightforward procedure. KTA is dissolved in methanol and well formed crystals are recovered as the solution slowly evaporates. However, the synthesis of **2** can be challenging because the aggregate structure is a metastable phase relative to the rod form under most conditions. Attempts to grow the acetic acid co-crystal (**2**) usually result in batches that contain only the rod form (**1**). There is constant competition from the more thermodynamically stable rod structure. One method of growing this crystal involves saturating 10 mL of glacial acetic acid with KTA (*ca.* 0.1 M). The solution is heated well to dissolve all traces of the rod form in the starting material. Left overnight, there appear well formed single crystals in the vial – but they are the rod form, not the aggregate structure. The thermodynamic product forms under equilibrium conditions. If this vial is given a sharp shock then a host of nucleation events occurs and the kinetic product grows over the course of a few hours. These small crystals can be used to seed a fresh batch of saturated solution, producing the aggregate structure as the predominant product. Kinetic conditions are used to nucleate and grow seed crystals of **2**, and the seeds can be used to grow **2** under thermodynamic conditions in glacial acetic acid.

Crystals of **2** that are isolated and placed in methanol will convert to the rod from overnight, confirming that the rod form of KTA is the thermodynamic product. Once isolated in the air, however, the crystals soon become opaque (Fig. 9) due to the loss of acetic acid from the lattice.

Conclusions

The carboxylic acid pair is an extremely common synthon in crystal engineering, but the occurrence normally involves two identical acid groups bonded across an inversion center. In this case, a dimer between KTA is formed with the traditional like–like carboxylic acid-pair synthon, but the interaction between the two remaining acid groups on each KTA molecule and acetic acid represents a relatively rare interaction because the pairing of un-like organic acids is uncommon. Typically, the pairing of like acids around inversion centers is favored.[11]

The stabilization of **2** in this kinetically controlled system is driven by the self-complementary shape of the aggregate working together with C–H···O interactions. These interactions are additive and with the efficient packing they are just able to edge out the formation of the basic rod form under appropriate conditions to afford the unique, though metastable, KTA–HOAc aggregate-based structure, **2**. The nucleation of **2** must be accomplished under kinetic control because under thermodynamic conditions the nucleation and growth of the rod is more frequently observed.

The co-crystal synthesis approach can be used to create crystalline materials in which the central molecule is obtained in a form that has properties that may be more appropriate for a particular application than the structure of the central molecule alone.

Table 2 Crystallographic data for **1** and **2**[a]

Parameter	**1**	**2**
Empirical formula	$C_{12}H_{18}O_6$	$C_{16}H_{26}O_{10}$
M	258.26	378.37
Crystal dimensions/mm	0.59 × 0.07 × 0.02	0.20 × 0.17 × 0.15
Crystal system	Monoclinic	Monoclinic
Space group	$P2_1/n$	$P2_1/n$
a/Å	8.3929(4)	12.0050(1)
b/Å	11.9975(6)	14.4584(1)
c/Å	12.8189(7)	12.0802(1)
α/°	90	90
β/°	101.517(1)	113.768(1)
γ/°	90	90
V/Å^3	1264.8(1)	1918.97(3)
Z	4	4
T/K	100(2)	100(2)
F(000)	552	808
λ/Å	0.71073	1.54178
θ Range/°	2.35–32.88	4.38–66.13
Max., min. transmission	1, 0.613	1, 0.912
Reflections collected	16 168	8999
Independent reflections	4456	3216
Data, restraints, parameters	4456, 0, 235	3216, 0, 339
Goodness-of-fit on F^2	1.074	1.047
Final *R* indices [$I > 2\sigma(I)$]	$R_1 = 0.0443$ $wR_2 = 0.0828$	$R_1 = 0.0310$ $wR_2 = 0.0822$
R indices (all data)	$R_1 = 0.0621$ $wR_2 = 0.0852$	$R_1 = 0.0341$ $wR_2 = 0.0843$

[a]Click here for full crystallographic data (CCDC 181092, 181093).

Experimental

KTA was purchased from Aldrich.

Crystallography of $[Me_3C_6H_6(COOH)_3]$ (1) and $[(Me_3C_6H_6(COOH)_3)(MeCOOH)_2]_2$ (2)

Data were collected at −173 °C on Bruker AXS D8 single-crystal X-ray diffractometers equipped with a SMART-APEX CCD area detector using Mo Kα graphite monochromated radiation for **1** and a SMART-1000 CCD area detector using Cu Kα graphite monochromated radiation for **2**. Scans were collected using 10 s frames traversing about ω at 0.3° increments. Data collection and cell refinement were performed using Bruker SMART[12] and SAINT[13] software, while data reduction was performed with Bruker SAINT software. The structures were determined using direct methods and refined by full-matrix, least squares methods (SHELXTL Ver. 5.10).[14] An empirical absorption correction for each data set was applied using the SADABS[15] program. Hydrogen atoms were found in the Fourier map and refined with isotropic thermal parameters. Additional details are found in Table 2.

Acknowledgements

NIH (S10 RR13673) & NSF (#CHE-9974864) supplied funds to purchase the diffractometers, and Emory University and the University Research Committee Emory University provided additional financial support.

Notes and references

1 G. Guilera and J. W. Steed, *Chem. Commun.*, 1999, 1563.
2 J. C. MacDonald, *Cryst. Growth Des.*, 2001, **1**, 29.
3 D. S. Kemp and K. S. Petrakis, *J. Org. Chem.*, 1981, **24**, 5140; J. Rebek Jr., B. Askew, M. Killoran, D. Nemeth and F.-T. Lin, *J. Am. Chem. Soc.*, 1987, **109**, 2426.
4 We have created 20 unique co-crystals containing KTA. Papers describing these results will appear in the literature. For pre-prints, contact the authors.
5 J. Rebek Jr., L. Marshall, R. Wolak, K. Parris, M. Killoran,

B. Askew, D. Nemeth and N. Islam, *J. Am. Chem. Soc.*, 1985, **107**, 7476.
6 T. L. Chan, Y. X. Cui, T. C. W. Mak, R. J. Wang and H. N. C. Wong, *J. Crystallogr. Spectrosc. Res.*, 1991, **21**, 297; A. Hazell and H. Toftlund, *Acta Crystallogr., Sect. C: Cryst. Struct. Commun.*, 1999, **55**, IUC9900079.
7 J. Perlstein and K. Steppe, *J. Am. Chem. Soc.*, 1996, **118**, 8433; J. J. Perlstein, *J. Am. Chem. Soc.*, 1994, **116**, 11 420.
8 D. Braga, A. Angeloni, E. Tagliavini and F. J. Grepioni, *J. Chem. Soc., Dalton Trans.*, 1998, 1961.
9 G. R. Desiraju, *Crystal Engineering: The Design of Organic Solids*, Elsevier, Amsterdam, 1989.
10 Scanning electron microscopy was performed at the Integrated Microscopy & Microanalytical Facility, Department of Chemistry, Emory University. Special thanks go to Dr Robert Apkarian for his assistance and expertise.
11 G. M. Frankenbach and M. C. Etter, *Chem. Mater.*, 1992, **4**, 272.
12 SMART Version 5.55, Bruker AXS, Inc., Analytical X-Ray Systems, 5465 East Cheryl Parkway, Madison, WI 53711-5373, 2000.
13 SAINT Version 6.02, Bruker AXS, Inc., Analytical X-Ray Systems, 5465 East Cheryl Parkway, Madison, WI 53711-5373, 1999.
14 SHELXTL Version 5.10, Bruker AXS, Inc., Analytical X-Ray Systems, 5465 East Cheryl Parkway, Madison, WI 53711-5373, 1997.
15 G. M. Sheldrick, SADABS, University of Göttingen, Germany, 1996.